Molecular Orientation of Hairy-Rod Polyesters: Effects of Side Chain Length

K. Andrikopoulos,[†,‡] D. Vlassopoulos,[*,§] and G. A. Voyiatzis[†]

Foundation for Research & Technology-Hellas (FORTH), 71110 Heraklion, Crete, Greece, Institute of Chemical Engineering and High-Temperature Chemical Processes, Box 1414, GR26500 Patras, Greece, and Institute of Electronic Structure & Laser, Box 1527, GR71110 Heraklion, Crete, Greece

Y. D. Yiannopoulos and E. I. Kamitsos

National Hellenic Research Foundation, Institute of Theoretical and Physical Chemistry, 48 Vas. Constantinou Avenue, GR11635 Athens, Greece

Received December 5, 1997

ABSTRACT: Polarized laser Raman microscopy was employed in order to investigate the effects of side chain length on the orientability of uniaxially drawn films of a model hairy-rod polymer, as a function of draw ratio; an aromatic polyester containing terphenyl units in the main chain and aliphatic side chains (hexyl and dodecyl units) was used in the experiments. The second and fourth moments of the segment orientation distribution function, P_2 and P_4, respectively, determined from the analysis of the Raman spectra, indicate that the polyester with longer (dodecyl) side chains clearly exhibits higher molecular orientation compared to the one with shorter (hexyl) side chains, for the same draw ratio. Complementary FTIR measurements provide detailed information on the segmental orientation and confirm the effects of side chain length in inducing orientation; the latter result strongly suggests that the longer aliphatic side chains are oriented toward the polyesteric main chain, much more effectively than the shorter ones, apparently due to their higher flexibility. Raman measurements at high wavenumbers corresponding to the CH_2 and CH_3 stretching modes of the aliphatic side chains corroborate this suggestion. Further evidence comes from independent measurements of optical anisotropy of *p*-phenylene oligomers bearing hexyl and dodecyl side chains. The implications to the processing of hairy polymers are evident.

I. Introduction

Molecular orientation in polymers is very important for controlling their processing behavior and tailoring the properties of the final products.[1,2] In the past decades significant advances have been made in the development of robust experimental methodologies for the accurate measurement of this important property.[1−15] Of particular interest is the application of Raman spectroscopy, mainly because of its ability to provide independent information on both the second ($\langle P_2(\cos\theta)\rangle = [3\langle\cos^2\theta\rangle - 1]/2$, with θ being the orientation angle) and the fourth ($\langle P_4(\cos\theta)\rangle = [35\langle\cos^4\theta\rangle - 30\langle\cos^2\theta\rangle + 3]/8$) moments of the expansion of the orientation distribution function,[3,5,7,11] referred to as P_2 and P_4, respectively. The analysis of the Raman scattering spectrum from a material, yielding the molecular orientation, dates back to the original work of Bower.[16] This analysis has been successfully employed in order to investigate the molecular orientation in a number of semicrystalline polymers, such as polyethylene[17,18] and PET.[5] Very recently, we have applied a slightly modified version of this analysis to hairy-rod polymers,[11] in order to unambiguously determine their molecular orientation as a function of draw ratio. Results have demonstrated the ability of this technique to detect the molecular orientation in polyester films and to distinguish this information from the larger-scale liquid crystalline domain orientation, typically detected with wide-angle X-ray scattering. On the other hand, the combination of Raman scattering with FITR is particularly powerful in obtaining unambiguously the orientation of different groups in the molecule.

Since the effects of drawing on the molecular orientation are rather well understood, the next challenge is to investigate the interplay between the macromolecular architecture and the molecular orientation at a given draw ratio. This is precisely the scope of this paper. We addressed this problem by concentrating on a well-characterized hairy-rod polyester, and to a first approach we investigated such systems with different hair size, i.e., different side chain length, and studied the orientation at various draw ratios. It is now well-established that one of the main functions of side chains is to improve the relatively poor processability of rigid-rod polymers (backbones only);[19] it is thus of particular importance to know what size of side chains will enhance the processing performance of these materials, and this actually represents a motivation for the present study. Due to the anticipated small difference in orientability between the two polymers (the only difference between them is the size of the side chains), it was desirable to obtain the highest possible accuracy from the Raman scattering measurements; to this end, we utilized a Raman miscroscopy technique,[20] which yielded accurate intensity data, with significantly reduced noise, compared to the measurements using conventional polarized Raman spectroscopy.[11]

This paper is organized as follows: Section II describes briefly the materials and techniques used, as well as a Raman analysis adapted to the backscattering configuration in order to determine P_2 and P_4; section

[†] Institute of Chemical Engineering and High-Temperature Chemical Processes.
[‡] Also at the Department of Chemical Engineering, University of Patras, GR26500 Patras, Greece.
[§] Institute of Electronic Structure & Laser.

S0024-9297(97)01773-7 CCC: $15.00
Published on Web 07/21/1998

Chart 1. Molecular Structure of PES1.3/C_6 and PES1.3/C_{12} Hairy-Rod Polyesters (n = Number of Repeat Units)

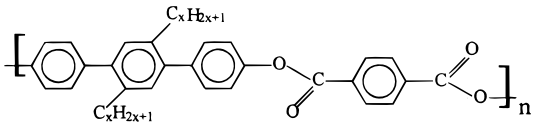

III discusses the results and evaluation of the effects of side chains and drawing on the molecular orientation; the main conclusions are then summarized in section IV.

II. Experimental Section

Materials. A model aromatic hairy-rod polyester (PES), with a main chain consisting of stiff terphenyl units and two kinds of flexible alkyl side chains, with six (hexyl, C_6) and twelve (dodecyl, C_{12}) carbons, respectively, was utilized; it was synthesized by a polycondensation technique.[21] This type of polyesters is typically denoted as PES*y.z*/C*x*, with *y* the number of phenylene rings in the diacid monomer, *z* the number of phenylene rings in the dihydroxy monomer, and *x* the number of carbon atoms in the side chain. The molecular structure of the polymers (coded as PES1.3/C_6 and PES1.3/C_{12}, respectively) is shown schematically in Chart 1. Typical molecular weights were about 30 000, based on intrinsic viscosity measurements, whereas the polydispersity index (M_w/M_n) was determined from GPC and found to be about 3.6 and 2.7 for the PES1.3/C_6 and PES1.3/C_{12} samples, respectively.[21] Although the glass transition temperature of such semistiff chains is not clearly resolved, usually it varies between 110 and 140 °C.[21] Films of nearly uniform thickness (of about 30 $\pm$ 2 μm) were obtained after casting an isotropic solution of ~6 wt % polymer in chloroform. Uniaxially oriented films were obtained by drawing the films in an oven at a temperature of about 270 °C for PES1.3/C_6 and 200 °C for PES1.3/C_{12}; this was recently confirmed by WAXS measurements.[19] The temperature was controlled by passing preheated dry nitrogen gas through the oven. The standard drawing speed was 2 cm/min, and the specimen length and width before drawing were 5 and 1 cm, respectively. The draw ratios achieved were between 1.5 and 3.9.[19,22] It is noted that the drawing temperatures were chosen as the ones corresponding to the maximum draw ratio achieved for each sample; this relates to the sample fragility and also suggests a higher orientability for PES1.3/C_{12}. Moreover, at these high temperatures the molecular relaxations are very fast compared to the drawing times.[22] The drawn films were immediately quenched (cold water), and thus any kinetic effects relating to molecular relaxations, which were not the subject of this investigation anyway, were not relevant.

Laser Raman Microscopy (LRM). The Raman spectra were excited with linearly polarized light; an air-cooled Ar^+ laser, was used with wavelength 514.5 nm (Spectra-Physics model 163-A42). A small-band-pass interference filter was used for the elimination of the laser plasma lines. The excitation beam was directed to a properly modulated sample compartment of a metallurgical microscope (Olympus BHSM-BH2). The microscope was used for the delivery of the excitation laser beam on the sample and the collection of the backscattered light through a beam splitter and the objective lens adapted to the aperture of the microscope. The focusing objective lens was a Long Working distance (8 mm) 50×/0.55 Olympus lens. For the polarization measurements, the following steps were followed: (i) on the excitation laser beam, a half wave plate was used to change the polarization direction; (ii) on the scattered beam, an analyzer permitted the selection of one component and a half wave plate was occasionally used, depending on the analysis geometry, to correct the polarization effect introduced by the gratings; and (iii) the spectra were corrected taking into account the beam splitter's dependence on the percent transmission and percent reflection due to polarization.

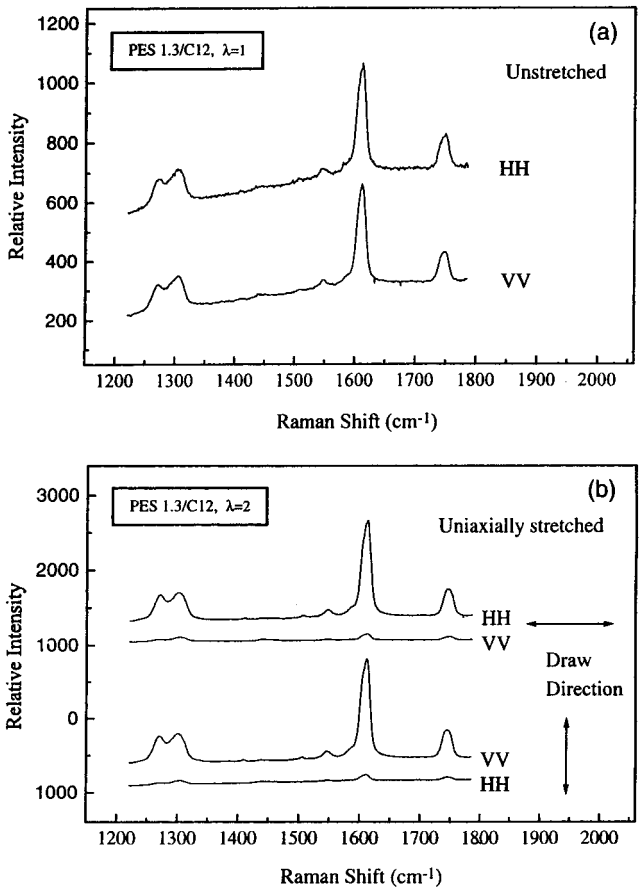

Figure 1. Polarized Raman spectra of PES3.1/C_{12} polyester films before (a) and after (b) uniaxial drawing (with draw ratio λ = 2), in two different polarization geometries with respect to the position of the specimen (relative to the laboratory-fixed coordinates), VV and HH. Vertical and horizontal arrows indicate the draw direction. The depolarization ratio indicates molecular orientation. The spectra are shifted along the intensity axis for clarity of presentation.

The spectra were obtained with a power of 3 mW on the specimen for a total integration time of 30 s. A viewing screen connected to the microscope offered good sample positioning, good laser beam focusing, and direct surface inspection. The scattered light was filtered through a holographic notch filter (HNF-514-1.0 from Kaiser Optical Systems), to remove the elastic Rayleigh scattering. The T-64000 (Jobin Yvon) Raman system, equipped with a Spectraview-2D liquid N_2-cooled CCD detector, was used, in the single spectograph configuration, to disperse and detect the Raman signal. The spectral resolution for the Raman spectra used for molecular orientation was ~5 cm^{-1}. The spectral window centered at 1500 cm^{-1} (in the Stokes region) was 587 cm^{-1} for 1022 valued pixels of the CCD detector. The Raman spectrum of the isotropic PES1.3/C_{12} polyesteric film, used for both the deconvolution procedure discussed below and the calibration adjustment of all Raman spectra, has been recorded with the FT-Raman FRA-106-S module of an Equinox 55 FTIR spectrometer of Bruker.

FTIR Spectroscopy. This technique was used as an independent probe of the molecular orientation, for comparison with the data obtained by Raman microscopy. Infrared spectra were measured in the transmission mode on a Bruker vacuum spectrometer (IFS 113v). The sample was mounted with its plane perpendicular to the incident infrared beam. A KRS-5 wire-grid polarizer was positioned before the sample to polarize the infrared radiation. The polarizer remained fixed and the sample was rotated by 90° in order to obtain transmission spectra with different polarization directions. The transmission spectrum of the polarizer was measured using the same instrument settings and was employed as the reference

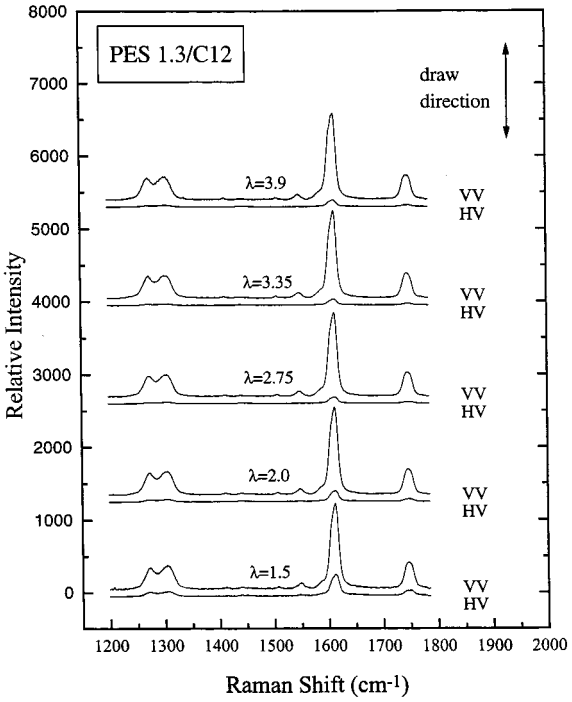

Figure 2. Coupled VV and HV polarized Raman spectra of polyester PES1.3/C_{12} films, uniaxially stretched (vertical arrow) at various draw ratios. Spectra are shifted along the vertical axis to avoid overlapping.

spectrum. All spectra were measured at room temperature and represent the average of 200 scans at 2 cm^{-1} resolution.

Results and Discussion

A. Raman Microscopy Measurements. Figure 1 depicts typical polarized Raman spectra from the PES1.3/C_{12} samples, before and after uniaxial drawing, in two different polarization geometries. First of all, it is noted that the Raman intensities are resolved very accurately and the level of noise is very low. It is clear that before drawing there is no preferred polarization, since the sample is essentially isotropic at a molecular level; thus, there is no difference between VV and HH scattering intensities. In contrast, when the sample is stretched, e.g., with a draw ratio $\lambda = 2$, there is a large difference between relative scattering intensities in the VV and HH polarizations, depending on the position of the sample with respect to the laboratory-fixed coordinates; this difference reflects the molecular orientation of the polyester, which is induced by the drawing process, and for this polymer it is more apparent at the Raman band of the para-disubstituted phenyl ring vibration,[11] situated at around 1609 cm^{-1}.

In Figure 2, coupled VV and HV polarized Raman spectra of PES1:3/C_{12} films are shown at various draw ratios. The spectra parallel to the drawing direction, VV, polarization geometry, have been normalized via the Raman peak intensity at 1609 cm^{-1}. In the corresponding HV polarized Raman spectra (of combined polarization geometry), we can clearly observe that with increasing draw ratio from $\lambda = 1$ to $\lambda = 2.75$, the intensity of the 1609 cm^{-1} vibrational band is continuously decreasing, indicating a molecular orientation increment; at higher draw ratio the depolarization ratio (HV/VV) levels off, suggesting that, for PES1:3/C_{12} films, the maximum possible orientation has been reached. In this figure, no shifts are observed in the various characteristic intensity peaks corresponding to

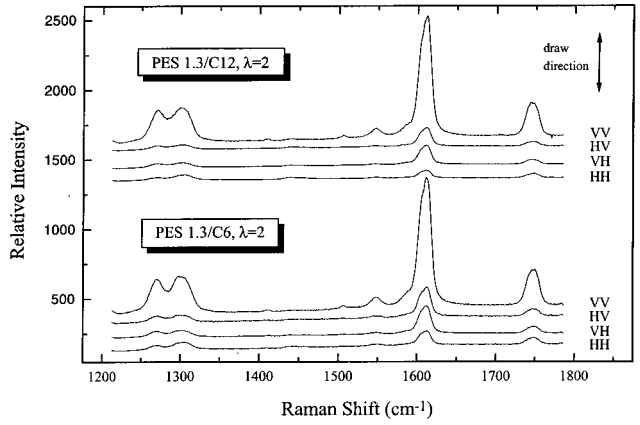

Figure 3. Raman spectra of polyester films PES1.3/C_6 and PES1.3/C_{12}, uniaxially stretched with draw ratio $\lambda = 2$, at various polarization geometries. The vertical arrow indicates the draw direction. The spectra are shifted vertically for clarity.

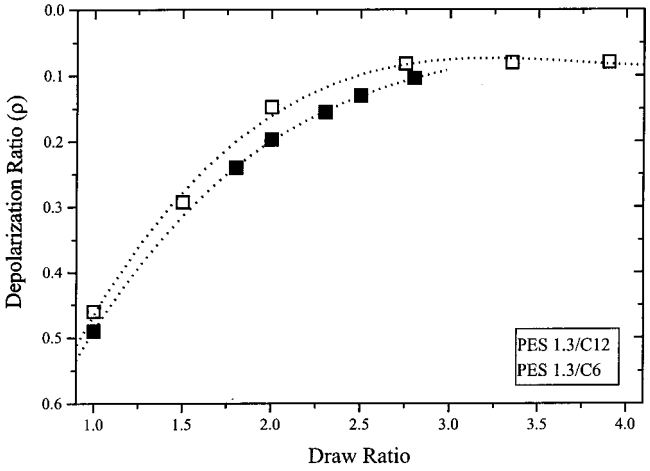

Figure 4. Depolarization ratio (ρ) of polyester films PES1.3/C_6 (■) and PES1.3/C_{12} (□) for the 1609 cm^{-1} phenyl ring Raman band, as functions of the draw ratio, for uniaxial stretching.

different Raman bands, and in particular the 1609 cm^{-1} of interest here, thus confirming that the molecular polarizabilities remain unchanged with orientation.

A first qualitative assessment of the effects of side chain length on the orientability of the polyester films can be made from Figure 3, which depicts the Raman spectra of PES1.3/C_6 and PES1.3/C_{12} at draw ratio $\lambda = 2$ in all four polarization geometries for a defined sample orientation. By concentrating again at the 1609 cm^{-1} Raman band, it seems that for the same draw ratio the depolarization ratio, $\rho = I_{HV}/I_{VV}$, for PES1.3/C_{12} is lower than for PES1.3/C_6.

This is clear in Figure 4 where the depolarization ratios for the 1609 cm^{-1} phenyl ring Raman band of both polyester films (PES1.3/C_6 and PES1.3/C_{12}) are shown as functions of the draw ratio, for uniaxial stretching.

All above observations suggest a higher molecular orientation of the polyesteric film with longer side alkyl chains. It should be noted that the Raman intensity distribution around the 1609 cm^{-1} line does not appear to be unique and its unambiguous resolution requires either deconvolution or/and comparison with corresponding Raman spectra of specified model polyesters, as will be discussed below.

B. FTIR Measurements. Typical polarized infrared absorption spectra are shown in Figure 5 for PES1.3/

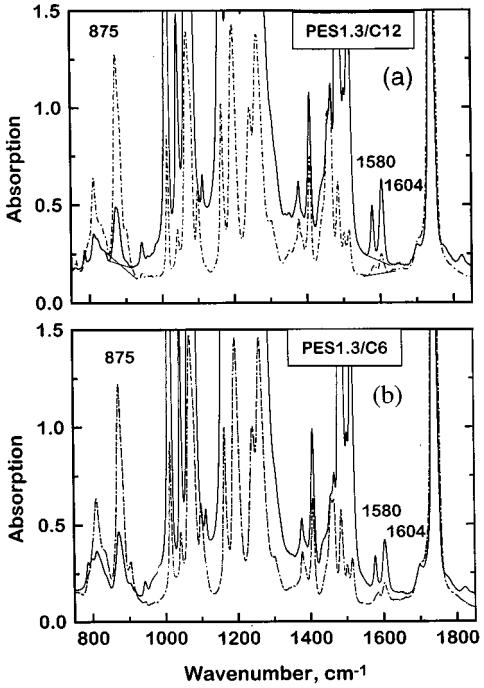

Figure 5. Polarized infrared absorption spectra of PES1.3/C_{12} (a) and PES1.3/C_6 (b) polyester films at draw ratio $\lambda = 2.75$. Solid lines represent polarization with the electric vector parallel to the stretching direction, whereas dashed lines represent polarization perpendicular to the stretching direction. Typical baselines for peaks at 875 cm^{-1} and the region 1580−1604 cm^{-1} are shown for (a).

C_{12} and PES1.3/C_6 polyester films with $\lambda = 2.75$. Most of the infrared bands exhibit saturation effects resulting mainly from the relatively large film thickness. Nevertheless, bands sensitive to orientation effects can be indentified and employed as probes of the induced molecular orientation. Such bands are those at ca. 1600 and 875 cm^{-1}.

In particular, the bands at 1580 and 1604 cm^{-1} were found to respond to film stretching and exhibit parallel polarization, as shown in Figure 5. Bands in the region of 1600 cm^{-1} are typically attributed to CC stretching vibrations of aromatic rings with parallel dichroism.[23] In our recent study of PES3.3/C_6 films it was found that the infrared active CC stretching vibrational mode of terphenyl-like rings appears at 1605 cm^{-1},[11] suggesting therefore the same origin for the 1604 cm^{-1} band of PES1.3 materials. The second band at 1580 cm^{-1} can be assigned to the CC stretching vibration of the PET-like ring of PES1.3, since PET exhibits the corresponding band at exactly the same frequency, and with parallel polarization.[24]

C. Analysis of Raman Spectra. To deduce P_2 and P_4, the backscattering geometry, depicted in Figure 6, was used. We have adopted the analysis of Pigeon et al.,[17] based on the theory of Bower[16] for the determination of the distribution of molecular orientation in oriented polymers from their Raman spectra. Two sets of coordinate axes are fixed, one referred to the sample, $Ox_1x_2x_3$ (or $Ox_1'x_2'x_3'$, when the sample is tilted by an angle u, as shown in Figure 6), and the second one to the experimental setup and the laboratory, $OX_1X_2X_3$. The total Raman scattering intensity is given by

$$I_s = I_o \sum (\sum I_i I_j' a_{ij})^2 \qquad (1)$$

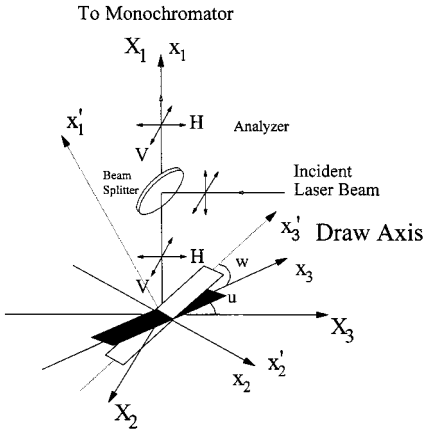

Figure 6. Coordinate axes for backscattering Raman geometry (see text for details).

I_i and I_j' are the polarization direction of the scattered and incident light with respect to the set of axes fixed in the sample.

The experimental values are of the form $I_o = \sum a_{ij} a_{pq}$ and in the case of uniaxial statistical symmetry with no preferred orientation one can write:

$$\sum a_{ij} a_{pq} = 4\pi^2 N_o \sum M_{l00} A_{l00}^{ijpq} \qquad (2)$$

M_{l00} is expressed in terms of Legendre polynomials:

$M_{l00} = (1/4\pi^2)\{(2\lambda + 1)/2\}^{1/2} \langle P_l(\cos\theta) \rangle$ ($l = 0, 2, 4$). A_{l00}^{ijpq} is a sum containing a_1, a_2, a_3. There are only five independent nonzero sums $\sum a_{ij} a_{pq}$ that are of the forms $\sum a_{ii} a_{jj}$ and $\sum a_{ij}^2$, in agreement with the analysis of Mead.[25] These are

$$\sum a_{22}^2 = xR_1 + yR_2 + 3zR_3 = I_{VV}(w = 0°, u = 0°) \qquad (3a)$$

$$\sum a_{33}^2 = xR_1 - 2yR_2 + 8zR_3 = I_{HH}(w = 0°, u = 0°) \qquad (3b)$$

$$\sum a_{32}^2 = xR_4 - yR_5 + 4zR_3 = I_{HV}(w = 0°, u = 0°) \qquad (3c)$$

$$\sum a_{22} a_{33} = xR_6 - yR_7 - 4zR_3 = \frac{I_{VV}(w = 0°, u = 0°)}{2} + \frac{I_{HH}(w = 0°, u = 0°)}{2} - 2I_{HV}(w = 0°, u = 45°) \qquad (3d)$$

$$\sum a_{12}^2 = xR_4 + 2yR_5 + zR_3 = I_{HV}(w = 90°, u = 0°) \qquad (3e)$$

We note I_{ij} as the experimentally observed intensity of the scattered light, when the incident light is polarized parallel to the j axis and the scattered light is polarized parallel to the i axis, fixed to the laboratory. R_i are second-order polynomials of $\alpha = a_1/a_3 = a_2/a_3$ (on the basis of literature evidence, in particular for the C1−

C4 aromatic vibrational band, we assume that we have a cylindrical Raman tensor, i.e., $a_1 = a_2$):[5,11]

$$R_1 = \frac{1}{15}(8a^2 + 4a + 3)$$

$$R_2 = \frac{1}{21}(8a^2 - 2a - 6)$$

$$R_3 = \frac{1}{280}(8a^2 - 16a + 8)$$

$$R_4 = \frac{1}{15}(a^2 - 2a + 1)$$

$$R_5 = \frac{1}{42}(-2a^2 + 4a - 2)$$

$$R_6 = \frac{1}{15}(6a^2 + 8a + 1)$$

$$R_7 = \frac{1}{42}(12a^2 - 10a - 2)$$

$x = b$ (an experimental parameter), $y = \langle P_2(\cos\theta)\rangle/b$, $z = \langle P_4(\cos\theta)\rangle/b$.

In the above equations (3a)−(3e) there are four unknowns x, y, z, and α. We have to use four of them in order to solve the system. Equation 3e cannot be used because the samples are practically two-dimensional. Thus there is no straightforward way to obtain a Raman signal from that geometry; of course, we could use another geometry with other values of the w angle, but that would increase the number of geometries needed and eventually involve mistakes due to birefringence effects (because of the tilting of the sample), as well as to bad focusing on the sample. Thus, there are four equations remaining with four unknowns. We would like to get rid of eq 3d because it is the one that is more affected by birefringence effects of our samples. There is another equation that gives directly the α in this case (under the hypothesis of a cylindrical Raman tensor), giving the opportunity to eliminate eq 3d that contains experimental mistakes. From the definition of the isotropic depolarization ratio, $\rho = (1 + \alpha^2 - 2\alpha)/(3 + 8\alpha^2 + 4\alpha)$, we can directly calculate α by measuring experimentally ρ of the isotropic (unstretched) sample as $\rho = I_{HV}/I_{VV}$.[11,14] Calculating α we then need three equations (3a)−(3c) which form a linear algebraic system, to determine the rest of the unknowns. This system has easily been solved analytically. It is noted in this context, that measurements of ρ at different angles in the level of the speciment (in which we measure the orientation; see Figure 6) confirmed that it is indeed isotropic.

The analysis of the Raman spectra can be summarized in Figure 7, where the three independent normalized intensity spectra for PES1.3/C_{12} are shown, corresponding to 1609 cm^{-1} and $\lambda = 2$. The ability to resolve even small intensities clearly relates to the reduced noise of the intensities measured with LRM. It is noted that deconvolution of the intensity spectrum between the 1590 and 1630 cm^{-1} lines yields for the actual 1609 cm^{-1} Raman band of interest the intensity distribution shown in Figure 8, obtained from an FT-Raman spectrum of the isotropic PES1.3/C_{12} polyesteric film. The deconvolution procedure that better explains the Raman findings of a series of model polyester

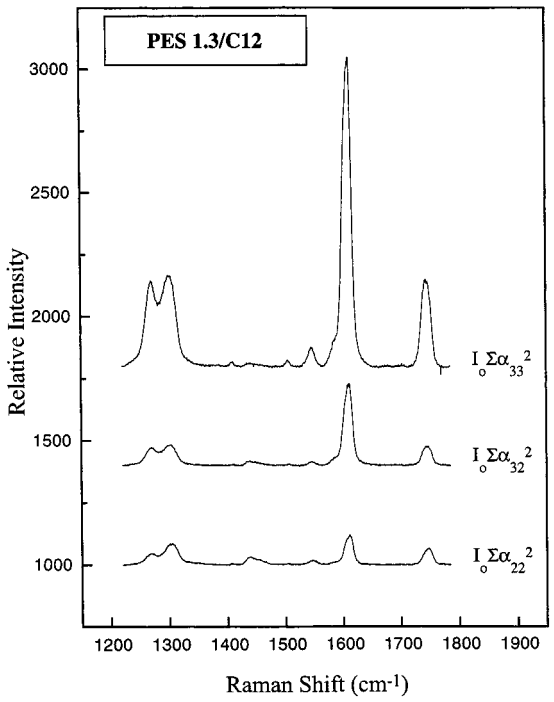

Figure 7. Typical normalized Raman intensities of the 1609 cm^{-1} benzene ring vibration band for PES1.3/C_{12} at draw ratio $\lambda = 2$, used for the determination of molecular orientation. The plots are shifted vertically for clarity.

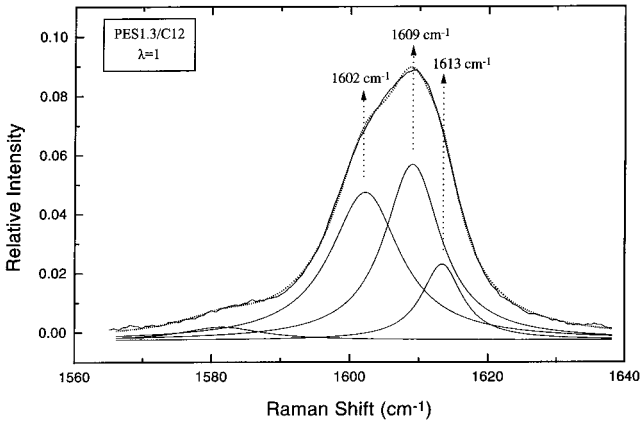

Figure 8. Typical deconvoluted (with three Lorentzians) FT-Raman spectrum of a polyesteric PES1.3/C_{12} film in the 1609 cm^{-1} Raman band intensity distribution. The three characteristic peaks are designated by vertical arrows.

compounds,[26] namely PES1.3/C_6, PES1.3/C_{12}, PES1.5/OC_{12}, PES1C_6/3C_{12}, PES1.3/OC_6, indicates a trimodal Raman intensity distribution around the 1609 cm^{-1} line: one Raman band situated at 1613 cm^{-1}, a second one around 1609 cm^{-1}, and a third one at about 1602 cm^{-1}. These three deconvoluted bands are attributed to the symmetrical stretching of para disubstituted mono- (PET-like) and terphenyl rings (side and centered para-phenyl ring, which exhibit the side chain substitution), respectively. It should be noted that for all polarization geometries used, at any actual draw ratio, the relative Raman intensity distribution at ~1609 cm^{-1} is nearly the same (see Figure 9). This result indicates that all three deconvoluted Raman bands are influenced to the same degree by any polarization measurement and by any molecular orientation achieved. Therefore, by this approach we can prove that our Raman analysis, based on 1609 cm^{-1} intensity distribution, remains unambiguous.

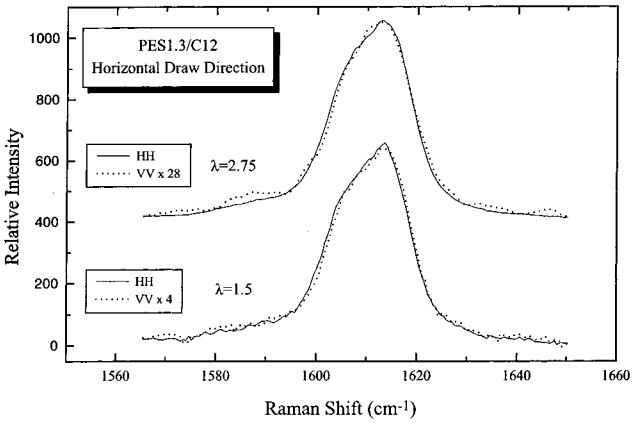

Figure 9. Comparison of Raman spectra (shifted vertically for clarity) obtained in the two crossed polarization geometries (VV, HH) and normalized at the same relative intensity for two PES1.3/C_{12} polyesteric films at different draw ratios.

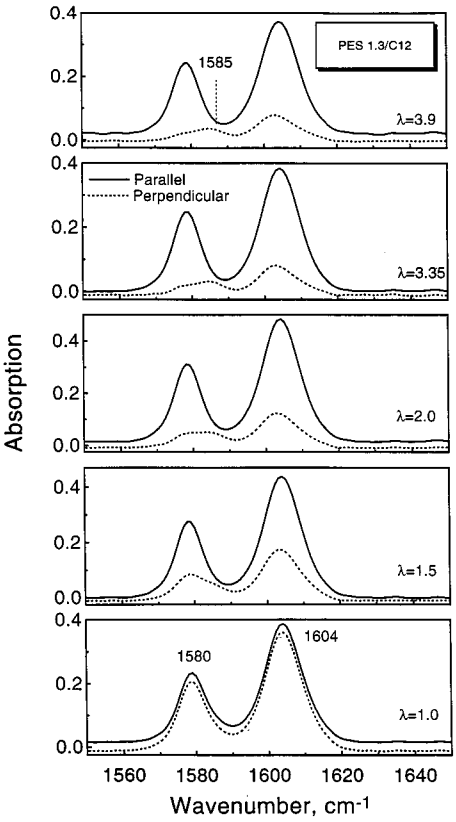

Figure 10. Polarized infrared absorption spectra of PES1.3/C_{12} films in the 1550−1650 cm^{-1} frequency range for various draw ratios. Solid and dotted lines represent polarization parallel and perpendicular to the stretching direction, respectively. The spectra with perpendicular polarization are slightly offset to facilitate comparison.

D. Analysis of FTIR Spectra. In the process of determining the dichroic ratio of the 1580 and 1604 cm^{-1} bands, it became evident that the band shape of the perpendicularly polarized spectra changes progressively upon increasing the draw ratio, λ. This is illustrated in Figure 10, where the polarized spectra of PES1.3/C_{12} samples are shown for various values of λ. For $\lambda = 1.0$, two identical spectra are measured with parallel and perpendicular polarization of the incident infrared beam. As λ increases, the intensity of the 1580 and 1604 cm^{-1} bands in the perpendicular spectra decreases and this allows a band at 1585 cm^{-1} to reveal its presence. This result indicates that the CC stretching region of the infrared spectrum is characterized by more than two bands. The polarized spectra of PES1.3/C_6 films were found to exhibit the same behavior.

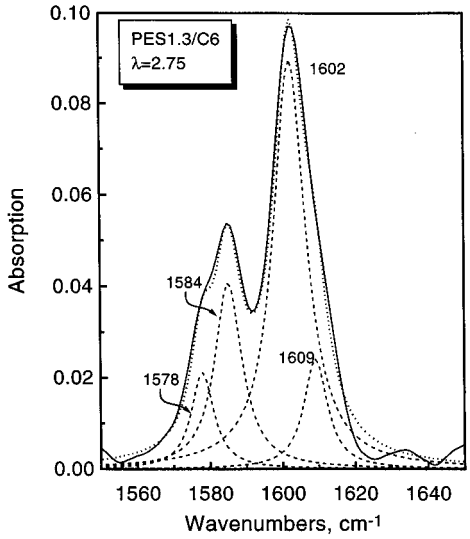

Figure 11. Example of spectral deconvolution of the 1550−1650 cm^{-1} range of a polyesteric film sample (PES1.3/C_6, $\lambda = 2.75$, perpendicular polarization). The measured spectrum (solid line) was deconvoluted into four Lorentzian bands (dashed lines), indicated by the characteristic wavenumbers. The simulated spectrum (dotted line) is also shown for comparison.

To explore this effect further, we have deconvoluted the 1550−1650 cm^{-1} region using a nonlinear least-squares program and the minimum number of bands that give a reasonable agreement between experimental and calculated spectra.[27] The functional form, the frequencies, bandwidths, and intensities are parameters adjustable by the program. An example of spectral deconvolution is depicted in Figure 11 for the PES1.3/C_6 $\lambda = 2.75$ sample measured with perpendicular light polarization. It was found that the 1550−1604 cm^{-1} profile of all spectra of PES1.3/C_{12}−C_6 samples could be well simulated with four Lorentzian bands having frequencies 1578 ± 0.5 cm^{-1}, 1584 ± 1.5 cm^{-1}, 1602 ± 0.5 cm^{-1}, 1609 ± 1 cm^{-1}, and corresponding bandwidths: 7 ± 0.5 cm^{-1}, 7 ± 1 cm^{-1}, 10 ± 1 cm^{-1}, and 7.5 ± 0.5 cm^{-1}.

Dichroic ratios, D, were calculated for the above bands using $D = A_{\parallel}/A_{\perp}$, where $A_{\parallel}$ and $A_{\perp}$ are the integrated absorptions obtained with incident radiation polarized parallel and perpendicular, respectively, to the draw direction. The obtained dichroic ratios (Figure 12) show that the CC stretching bands at 1578 and 1602 cm^{-1} have parallel polarization, as expected. These results are in agreement with the Raman depolarization ratios. The λ dependence of D for the latter bands (Figure 12a) provides direct evidence for the development of molecular orientation along the stretching direction. It was also found that D for the component at 1609 cm^{-1} has almost the same value as that of the 1602 cm^{-1} band for both PES1.3/C_{12} and PES1.3/C_6 films, indicating the same origin for these bands. The fourth band at 1584 cm^{-1} was the only one in the 1550−1650 cm^{-1} region exhibiting a weak perpendicular polarization, but since its assignment remains rather ambiguous,[23] it is not discussed further.

What is of particular interest from the findings in Figure 12a is the fact that D for the 1578 cm^{-1} band shows a very weak dependence on the side chain length,

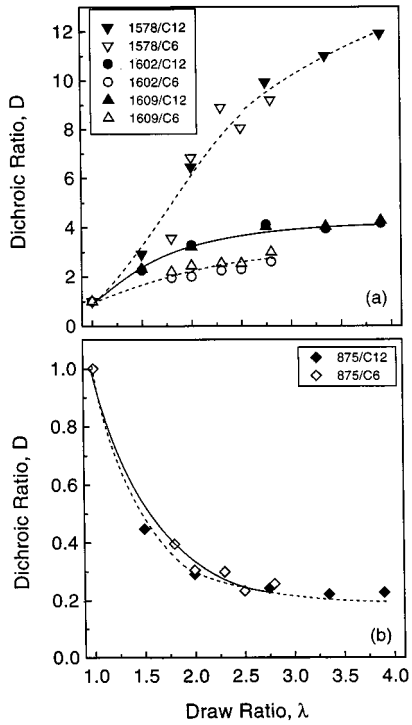

Figure 12. (a) Dichroic ratio, D, of infrared probe bands as a function of the macroscopic draw ratio. Lines are drawn to guide the eye. Bands at 1578 (inverted triangles), 1602 (circles), and 1609 (up triangles) cm^{-1} were obtained by deconvoluting the 1550−1650 cm^{-1} spectral region (Figure 11). The short notation C_{12} and C_6 refers to PES1.3/C_{12} (solid symbols) and PES1.3/C_6 (open symbols), respectively. (b) Corresponding D of the 875 cm^{-1} band for PES1.3/C_{12} (solid symbols) and PES1.3/C_6 (open symbols), respectively. Lines are drawn to guide the eye.

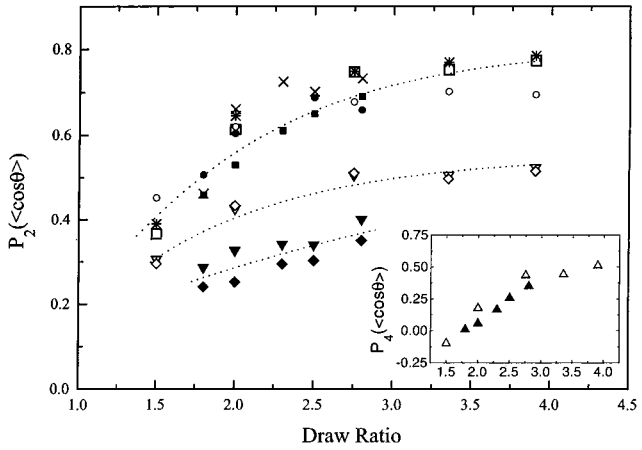

Figure 13. Second moment, P_2, of the orientation distribution function of polyester films PES1.3/C_6 and PES1.3/C_{12}, from Raman and FTIR, as a function of the draw ratio. Lines are drawn to guide the eye. PES1.3/C_{12}: (□) P_2-Raman, 1609 cm^{-1}; (○) P_2-FTIR, 875 cm^{-1}; (▽) P_2-FTIR, 1609 cm^{-1}; (◇) P_2-FTIR, 1602 cm^{-1}; (*) P_2-FTIR, 1578 cm^{-1}). PES1.3/C_6: (■) P_2-Raman, 1609 cm^{-1}; (●) P_2-FTIR, 875 cm^{-1}; (▼) P_2-FTIR, 1609 cm^{-1}; (◆) P_2-FTIR, 1602 cm^{-1}; (×) P_2-FTIR, 1578 cm^{-1}. Inset: Fourth moment, P_4, of the orientation distribution function of polyester films PES1.3/C_6 (▲) and PES1.3/C_{12} (△), determined from Raman measurements, as a function of the draw ratio.

as opposed to the behavior of D for the 1602 and 1609 cm^{-1} bands. In particular, the dichroic ratios for the latter bands are clearly larger for the C_{12} than for the C_6 films, suggesting that larger side chains induce a higher degree of molecular orientation. Such trends can be understood if we recall the origin of the bands in question, i.e., that the 1578 cm^{-1} band characterizes the PET-like ring, while the ones at 1602 and 1609 cm^{-1} characterize the therphenyl-like part of PES1.3, which is bonded to the side chains. It appears, therefore, that the 1578 cm^{-1} normal mode of the PET-like part of the polymer is not influenced by the length of the particular side chains.

We now focus attention on the infrared probe located at 875 cm^{-1} (Figure 5). Bands in this region are unambiguously assigned to the CH out-of-plane bending vibration of the benzene-like rings with a transition dipole moment developing perpendicular to the plane of the ring.[23,28] Indeed, the infrared spectrum of PES3.3/C_6 films exhibits two bands at 860 and 880 cm^{-1} for the CH out-of-plane bending vibration of the terphenyl-like rings with perpendicular polarization.[11] In addition, PET gives the corresponding mode at 875 cm^{-1} with the same polarization.[24] Thus, we suggest that the 875 cm^{-1} band of PES1.3 materials results from the combined contribution of the corresponding modes of the terphenyl-like and PET-like rings of the polyester. While the intensity of the 875 cm^{-1} band is very sensitive to polarization of infrared radiation, its shape remains practically unaffected by polarization and film stretching. Thus, we have obtained the dichroic ratio for this band using the baseline method[29] and show the results in Figure 12b. It is observed that D decreases with λ and shows a small dependence on the side chain length. Considering the polarization characteristics of the 875 cm^{-1} band, the findings in Figure 12b demonstrate again the induced molecular orientation upon uniaxial film stretching.

The quantification of molecular orientation on the basis of the infrared data requires calculation of the second-order Legendre polynomial, P_2, in terms of the dichroic ratio:[11,23]

$$P_2 = 2(D - 1)/(D + 2)(3\cos^2\psi - 1) \qquad (4)$$

where ψ is the angle between the direction of the vibrational transition moment and the polymer chain axis. It is quite reasonable to use $\psi = 90°$ for the 875 cm^{-1} band,[23] but there are cases where ψ is known to deviate from 90°. For example, $\psi = 85°$ for poly(*p*-benzamide) liquid crystals, and $\psi = 86°$ for PET.[28] It can be easily shown (eq 4) that reduction of ψ by 15° from the right angle results in an increase of P_2 by only 2%. Thus, we may assume an average value of $\psi = 90°$ for the PES1.3 polyesters and calculate P_2 using eq 4 and the measured D for the 875 cm^{-1} band. The obtained P_2 values (Figure 13) are very close to those of the Raman analysis.

E. Molecular Orientation and the Effects of Side Chains. The compiled orientation data obtained for the two polyesters, PES1.3/C_6 and PES1.3/C_{12}, are presented in Figure 13. First of all, a good agreement between the Raman and FTIR results is noted with respect to the observed trends. Further, the fact that the obtained trends in P_2 (and P_4) with draw ratio are consistent with the directly measured respective depolarization (or dichroic) ratios strongly suggests that, despite the experimental error, the analysis based on the assumptions of uniaxial symmetry of the drawn material and cylindrical symmetry of the Raman polarizability tensor are clearly unambiguous. The details and implications of the results, however, require further discussion.

In particular, concerning the FTIR results, it is noted that orientation data for the PES1.3 polyesters are obtained also using the dichroic ratios of the CC ring stretching modes at 1578, 1602, and 1609 cm^{-1}, for which assignments are quite certain. However, the values of angle ψ for these modes are not known for the polyesters under investigation, but we can assume that $\psi \approx 0°$.[11,23] It is noted though that deviations of ψ from 0° will cause a considerable effect on P_2. As an example, we indicate that P_2 obtained for $\psi = 0°$ is smaller by 11% than the P_2 value obtained for $\psi = 15°$ and for the same D value. Due to the absence of knowledge on the exact values of ψ we assume that $\psi = 0°$ and calculate P_2 for the 1578, 1602, and 1609 cm^{-1} bands. In any case, this assumption will not affect the trends of the orientation function with draw ratio, to which we mainly focus attention. The results shown in Figure 13 seem to suggest that the PET-like segments (1578 cm^{-1} band) are more effectively oriented than the terphenyl-like segments (1602, 1609 cm^{-1} bands) for both types of polyester films. Also, the orientation of the terphenyl-like segments appears clearly enhanced when larger side chains are bonded to them, in agreement with the Raman results.

The overall form of the P_2 versus draw ratio plots of Figure 13 suggests that the orientation behavior of these hairy-rod polyesters can be represented by the affine deformation model of Kratky.[30] Indeed, this model compares well both qualitatively and quantitatively with the obtained P_2 data, and thus it can represent to a good approximation the orientation of rigid rods in a viscous matrix, suggesting that elongation (rather than shear) may be the dominant mechanism of orientation during the drawing deformation.[11,19] However, as already pointed out in ref 11, its detailed evaluation is not truly meaningful, since it is based on principles of continuum mechanics and does not contain molecular parameters; thus it does not provide hints on the molecular origins of the orientation mechanism.

By comparing the results of Figure 13, it is also noted that the P_2 values determined from Raman and FTIR exhibit a distinct difference, beyond the respective experimental errors. We believe that this difference can be attributed to the fact that, whereas both techniques determine molecular orientation, they probe essentially different characteristics of the molecule, with corresponding different sensitivity to various experimental and drawing parameters: Raman probes the polarizability tensor and FTIR probes the dipole moments of the molecule. It is encouraging and important to note that P_2 from both techniques follows the same qualitative trend. Further, the above-mentioned assumption concerning cylindrical symmetry of the Raman polarizability tensor may not be entirely true, contributing thus to the descrepency between data (for the FTIR data this assumption is not relevant; see analysis of FTIR data above). It should be also noted that, as a consistency check, the P_4 values from the Raman data fall within the acceptable range for a given value of P_2, as determined by Bower for uniaxially stretched polymers.[11,31] Moreover, in agreement with the depolarization and dichroic ratios (Figures 4 and 12), above a value of draw ratio of about 2.5, both P_2 and P_4 (inset of Figure 13) reach a plateau, which appears to be the maximum orientation reached by these polyesters. The effects of side chain length on the P_2 of the terphenyl-like segments are substantial; based on Figure 13, the difference in P_2 (FTIR) can be as high as 0.18. On the other hand, the difference in orientation (Raman P_2 or P_4) between PES1.3/C_6 and PES1.3/C_{12} is small (amounting to about 0.08 in the whole range of draw ratios investigated), but still unambiguous and beyond experimental error. This strongly suggests that PES1.3/C_{12} orients more and easier than PES1.3/C_6; therefore, the longer side chains apparently enhance the orientability (and, thus, the processability) of the aromatic polyesters. This means that in the two polyester samples, PES1.3/C_{12} and PES1.3/C_6, the side chains have a different conformation with respect to the polymeric backbone. Such an idea seems reasonable, since a dodecyl chain is more flexible than a hexyl one, and thus the implied (from the data) conformation of the polyester with parallel arrangement of the C_{12} side chains (with respect to the main chain) is possible indeed. On the other hand, the hexyl chain is short enough and can be considered rather stiff, and thus it should not be able to realize a conformation parallel to the polyester main chain. To confirm this, we extended the Raman measurements to high wavenumbers, in the spectral window of 2800−3000 cm^{-1} corresponding to the characteristic CH_2 and CH_3 stretch modes of the aliphatic side chains (Figure 14). It has to be noted that, e.g., the CH_2 symmetrical stretching, at ∼2850 cm^{-1}, vibrates perpendicular to the aliphatic chain plane. As clearly seen in the inset of Figure 14 (for the typical case of $\lambda = 2.8$), the depolarization ratio ($\rho = I_{HH}/I_{VV}$) of the C_{12} aliphatic side chain is significantly larger than that of the C_6 one, implying higher orientation (with respect to the polyesteric backbone) of the former. A further supporting evidence comes from the optical anisotropy of various *p*-phenylene oligomers.[32] It was determined from depolarized Rayleigh scattering measurements in chloroform, in dilute solution; these oligomers consisted of systems without side chains but different lengths of main chain, and with the same main chain but with side alkyl chains of two different sizes, namely hexyls and dodecyls. From the results[32] it is evident that in the absence of side chains, increasing the length of the oligomeric backbone makes the material more anisotropic, as expected; but the optical anisotropy is not

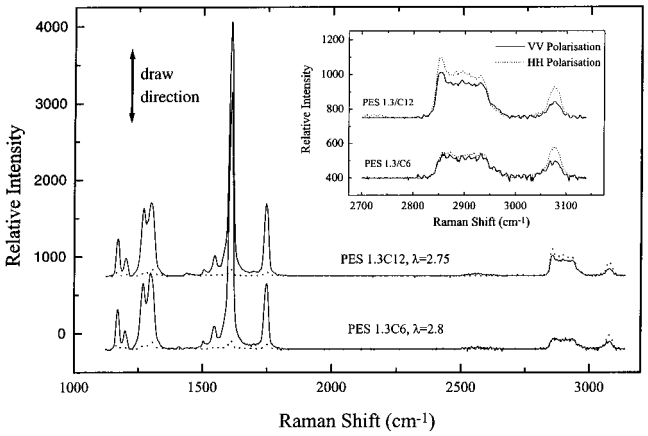

Figure 14. Raman spectra at a wide range of wavenumbers and different polarization geometries (HH, dotted lines, and VV, solid lines), indicating the orientability of the aliphatic side chains (PES1.3/C_{12} versus PES1.3/C_6), which have a characteristic "signature" at the high wavenumbers. The vertical arrow indicates the draw direction. For clarity, the spectra are offset along the intensity axis. Inset: details of the high-wavenumber Raman spectra of the aliphatic side chains, indicating clearly the higher depolarization ratio of the longer dodecyl chains.

linearly dependent on the molecular aspect ratio. What is more striking, however, is the finding that the oligomers with longer side chains (3.12) have higher anisotropy (by about 30%) than those with shorter side chains (3.6) and the same backbone, in harmony with the results from Figure 13. Thus, the dodecyl side chains lie roughly toward the main chain, whereas this is not possible, at least to the same extent, for the shorter (and stiffer) hexyl chains.

As a final comment, the molecular orientation results presented here, obtained with Raman microscopy (as well as FTIR spectroscopy), are qualitatively consistent with the wide-angle X-ray diffraction (WAXD) data on the same polyesters, reported recently by Bruggeman and Buijs;[19] these authors found higher values of orientation (P_2) for both PES1.3/C_6 and PES1.3/C_{12}, compared to our Raman and FTIR data, but this is already explained[11,19] as being due to the characteristic scale that each technique probes, i.e., molecular versus larger-scale crystalline domain orientation, for Raman and WAXD, respectively. The interesting result, however, which is not discussed in their paper, is that even the WAXD data show a higher orientation for the PES1.3/C_{12} polyester; compared to PES1.3/C_6, this strongly suggests that the oriented domains or layered structures of PES1.3/C_{12} are more anisotropic than those of PES1.3/C_6, apparently due to the higher anisotropy of the domain units (single macromolecules).

IV. Conclusions

Model aromatic polyesters bearing hexyl and dodecyl side chains were used in order to investigate the effects of side chain length on the orientability of uniaxially drawn films of hairy-rod polymers. The molecular orientation was probed effectively with a combination of polarized laser Raman microscopy and FTIR spectroscopic measurements. The measured second and fourth moments of the segment orientation distribution functions show that increasing the side chain length yields higher molecular orientation, and thus more efficient processability. This result is supported by Raman measurements at higher wavenumbers and results from optical anisotropy measurements,[32] which suggest that the conformation of the dodecyl side chains is toward the backbone of the polyester, in contrast to the situation with hexyl chains. Moreover, this effect of side chains on molecular orientation seems to persist at a larger-scale orientation of crystalline domains, probed with WAXD.[19] Finally, this work demonstrates that Raman microscopy provides more accurate information on orientation than the classical Raman spectroscopy,[11] due to the significantly better conditions of alignment and focusing and hence better measurements in different polarization geometries.

Acknowledgment. We are grateful to Mr. A. Bruggeman from the TNO Institute of Industrial Technology, The Netherlands, for kindly providing the polyester films used in this work. This work was partially supported by two grants from the Greek General Secretariat for Research and Technology (GSRT, Oriented Research Program 1996-99, YPER-375 and GSRT, Basic Research Program 1996-98, PENED-40).

References and Notes

(1) Ward, I. M. *Developments in Oriented Polymers − I, II*; Applied Science Publishers: London, 1982. Ward I. M. *Advances in Polymer Science*; Springer-Verlag: Berlin, 1985; Vol. 66, p 81.

(2) Wegner, G. *Mol. Cryst. Liq. Cryst.* **1993**, *235*, 1. Ballauff, M. In *Materials Science and Technology*; Cahn, R. W., Haasen, P., Kramer, E. J., Eds.; VCH: Weinheim, 1993. Ballauff, M. *Angew. Chem.* **1989**, *28*, 253.

(3) Lafrance, C−P.; Prud'homme, R. E. *Polymer* **1994**, 35, 3927. Gustafsson, G.; Inganas, O.; Osterholm, H.; Laakso, J. *Polymer* **1991**, 32, 1574.

(4) Jasse, B.; Tassin, J. F.; Monnerie, L. *Prog. Colloid Polym. Sci.* **1993**, *92*, 8. Kaito A.; Kyotani, M.; Nakayama, K. *J. Polym. Sci. B: Polym. Phys.* **1993**, *31*, 1099.

(5) Purvis, J.; Bower, D. I. *Polymer* **1974**, 15, 645. Purvis J.; Bower D. I. *J. Polym. Sci., Polym. Phys. Ed.* **1976**, *14*, 1461.

(6) Buffeteau, T.; Desbat, B.; Besbes, S.; Nafati, M.; Bokobza, L. *Polymer* **1994**, *35*, 2538.

(7) Archer, L. A.; Fuller, G. G.; Nunnelley, L. *Polymer* **1992**, *33*, 3574. Archer, L. A.; Fuller, G. G. *Macromolecules* **1994**, *27*, 4359.

(8) Lafrance, C−P.; Chabot, P.; Pigeon, M.; Prud'homme, R. E.; Pezolet, M. *Polymer* **1993**, *34*, 5029.

(9) Satija, S. K.; Wang, C. H. *J. Chem. Phys.* **1978**, *69*, 2739.

(10) Robinson, M. E. R.; Bower, D. I.; Maddams, M. F. *J. Polym. Sci., Polym. Phys. Ed.* **1978**, *16*, 2115. Lauchlan, L.; Rabolt, J. F. *Macromolecules* **1986**, *19*, 1049.

(11) Voyiatzis, G.; Petekidis, G.; Vlassopoulos, D.; Kamitsos, E. I.; Bruggeman, A. *Macromolecules* **1996**, *29*, 2244.

(12) Purvis, J.; Bower, D. I.; Ward, I. M. *Polymer* **1973**, *14*, 398.

(13) Jasse, B.; Koenig, J. L. *J. Polym. Sci. Polym. Phys. Ed.* **1978**, *16*, 2115.

(14) Li, W.; Prud'homme, R. E. *Polymer* **1994**, *35*, 3260. Abtal, E.; Prud'homme, R. E. *Polymer* **1993**, *34*, 4661.

(15) Kaito, A.; Nakayama, K.; Kyotani, M. *J. Polym. Sci. B: Polym. Phys.* **1993**, *29*, 1321.

(16) Bower, D. I. *J. Polym. Sci., Polym. Phys. Ed.* **1972**, *10*, 2135.

(17) Pigeon, M.; Prud'homme, R. E.; Pezolet, M. *Macromolecules* **1991**, *24*, 5687.

(18) Citra, M. J.; Chase, D. B.; Ikeda, R. M.; Gardner, K. H. *Macromolecules* **1995**, *28*, 4007.

(19) Bruggeman, A.; Buijs, J. A. H. M. *Polymer* **1996**, *37*, 5639.

(20) Turrell, G.; Corset, J., Eds. *Raman Microscopy. Developments and Applications*; Academic Press: London, 1996.

(21) Tiesler, U.; Pulina, T.; Rehahn, M.; Ballauff, M. *Mol. Cryst. Liq. Cryst.* **1994**, *243*, 299. Tiesler, U. Ph.D. Thesis, University of Karlsruhe, 1994. Kallitsis, J. D.; Rehahn, M.; Wegner, G. *Makromol. Chem.* **1992**, *193*, 1021.

(22) Damman, S. B.; Mercx, F. P. M.; Lemstra, P. J. *Polymer* **1993**, *34*, 2726.

(23) Colthup, N. B.; Daly, L. H.; Wiberley, S. E. *Introduction to Infrared and Raman Spectroscopy*; Academic Press: New York, 1975. Kaito, A.; Kyotani, M.; Nakayama, K. *Macromolecules* **1991**, *24*, 3244.

(24) Bahl, S. K.; Cornell, D. D.; Boerio, F. J.; McGraw, G. E. *J. Polym. Sci., Polym. Lett. Ed.* **1974**, *12*, 13. Boerio, F. J.; Bahl, S. K.; McGraw, G. E. *J. Polym. Sci., Polym. Phsys. Ed.* **1976**, *14*, 1029.

(25) Mead, D. W. Personal communication, 1996.

(26) Adrikopoulos, K.; Kallitsis, J. D.; Voyiatzis, G. A.; Vlassopoulos, D. Unpublished data.

(27) Kamitsos, E. I.; Yiannopoulos, Y. D.; Jain, H.; Huang, W. C. *Phys. Rev. B* **1996**, *54*, 9775.

(28) Cunningham, A.; Ward, I. M.; Willis, H. A.; Zichy, V. *Polymer* **1974**, *15*, 749. Sartirana, M. L.; Marsano, E.; Bianchi, E.; Ciferri, A. *Macromolecules* **1986**, *19*, 1176.

(29) Jabarin, S. A. *Polym. Eng. Sci.* **1991**, *31*, 638. Stein, R. S. *J. Polym. Sci.* **1958**, *31*, 335. Krimm, S. *J. Polym. Sci.* **1964**, C7.

(30) Kratky, O. *Kolloid Z.* **1942**, *101*, 248.

(31) Bower, D. I. *J. Polym. Sci., Polym. Phys. Ed.* **1981**, *19*, 93.

(32) Petekidis, G.; Vlassopoulos, D.; Galda, P.; Rehahn, M.; Ballauff, M. *Macromolecules* **1996**, *29*, 8948.

MA971773J